

EPJ D

Atomic, Molecular,
Optical and Plasma Physics

EPJ.org

your physics journal

Eur. Phys. J. D (2016) 70: 107

DOI: [10.1140/epjd/e2016-70148-y](https://doi.org/10.1140/epjd/e2016-70148-y)

Lowest autodetachment state of the water anion

Karel Houfek and Martin Čížek

edp sciences



 Springer

Lowest autodetachment state of the water anion^{*}

Karel Houfek and Martin Čížek^a

Institute of Theoretical Physics, Faculty of Mathematics and Physics, Charles University in Prague, V Holešovičkách 2, 180 00 Prague, Czech Republic

Received 29 February 2016 / Received in final form 18 March 2016

Published online 12 May 2016 – © EDP Sciences, Società Italiana di Fisica, Springer-Verlag 2016

Abstract. The potential energy surface of the ground state of the water anion H_2O^- is carefully mapped using multireference CI calculations for a large range of molecular geometries. Particular attention is paid to a consistent description of both the $\text{O}^- + \text{H}_2$ and $\text{OH}^- + \text{H}$ asymptotes and to a relative position of the anion energy to the ground state energy of the neutral molecule. The autodetachment region, where the anion state crosses to the electronic continuum is identified. The local minimum in the direction of the $\text{O}^- + \text{H}_2$ channel previously reported by Werner et al. [J. Chem. Phys. **87**, 2913 (1987)] is found to be slightly off the linear geometry and is separated by a saddle from the autodetachment region. The autodetachment region is directly accessible from the $\text{OH}^- + \text{H}$ asymptote. For the molecular geometries in the autodetachment region and in its vicinity we also performed fixed-nuclei electron-molecule scattering calculations using the R -matrix method. Tuning of consistency of a description of the correlation energy in both the multireference CI and R -matrix calculations is discussed. Two models of the correlation energy within the R -matrix method that are consistent with the quantum chemistry calculations are found. Both models yield scattering quantities in a close agreement. The results of this work will allow a consistent formulation of the nonlocal resonance model of the water anion in a future publication.

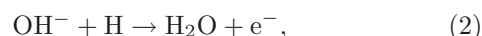
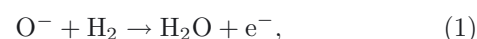
1 Introduction

Water is almost omnipresent in laboratory, environment and space. In fact it is the third most common molecule in space (after H_2 and CO) [1]. The low-energy electron scattering from the H_2O molecule plays an important role in the understanding of gas discharges, molecular clouds in space and atmospheres of planets, comets and even cold stars. Because of abundance of water in living tissue the reactive low-energy electron collisions with the water molecule represent an important step in the radiation damage of cells. Both the theoretical and experimental cross sections for various processes in the electron- H_2O collisions have been reviewed by Itikawa and Mason [1]. Here we begin with a short review focussing on electron energies below 5 eV and we point out some of the unresolved issues considering the role of the ground electronic state of H_2O^- .

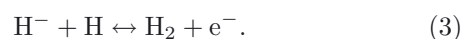
Let us start with the dissociative attachment (DA) process in which the electron is attached to the water molecule which is dissociated to the H^- , O^- or OH^- anions. This process has been studied both experimentally and theoretically for more than 50 years (see [2] for

comprehensive review). It was found that DA proceeds through the Feshbach resonances at electron energies near 6.5 ($^2\text{B}_1$), 8.6 ($^2\text{A}_1$) and 11.8 ($^2\text{B}_2$) eV [3,4]. The detailed analysis of the relevant potential energy surfaces (PES) and the nuclear dynamics within the local complex potential model has been done by Haxton et al. (see [2,5,6] and references therein). The PES of the ground electronic state of the anion ($^2\text{A}'$ in C_s symmetry or $^2\text{A}_1$ in C_{2v}) is not involved in these studies. This state exists as a bound state for geometries largely distorted from the equilibrium structure of the neutral H_2O molecule, but it disappears in the electronic continuum for configurations close to the equilibrium geometry [7]. This state could be involved in the DA process at lower electron energies (the thresholds for the production of OH^- , O^- and H^- are 3.27, 3.56 and 4.35 eV respectively) but no noticeable DA signal is measured for electron energies below 5 eV [3,4,8].

It is in contrast with the measurement of the associative detachment (AD) cross sections



which are large near the threshold [9–12]. This seems to be in contradiction since the AD and DA processes are closely related by the detailed balance principle. The resolution of the apparent paradox is well known from a similar situation in the AD process



^{*} Contribution to the Topical Issue “Advances in Positron and Electron Scattering”, edited by Paulo Lima-Vieira, Gustavo Garcia, E. Krishnakumar, James Sullivan, Hajime Tanuma and Zoran Petrovic.

^a e-mail: Martin.Cizek@mff.cuni.cz

In both systems the AD reaction proceeds very efficiently at low energies and it is known that it releases electrons with small energies [10,13], which means that emerging molecules must be highly excited. The DA reaction is very slow when calculated (or measured) with molecules in the ground state, but the cross section increases fast with the vibrational quantum number of the target molecule. While for the H_2 system this behavior is proved both by experiment [14] and theory [15], for the water molecule we can only assume that the DA process at the threshold will be activated by heating the target molecule.

The water molecule has a strong dipole moment of 1.85 D. This fact has a large influence on inelastic scattering of low-energy electrons. It is known that the molecule can be excited efficiently both rotationally [16] and vibrationally [17] by low energy electrons. It was even found that the vibrational excitation (VE) is most efficient for electron energies close to the threshold [18,19]. A similar situation is known from electron scattering from hydrogen halide molecules [20] where such threshold peaks have also been observed [21,22]. A very accurate description of these structures was achieved with the projection operator technique [23] which leads to the nonlocal resonance model [24,25] for nuclear dynamics. This technique can very efficiently account for the coupling between electronic and vibrational degrees of freedom due to the crossing of a discrete (anion) state to the continuum. This discrete state represents a bound state disappearing in the continuum, where it turns into a resonance or (as it happens in the case of the hydrogen halides) to a virtual state. The construction of a similar model for triatomic molecules like H_2O has not yet been achieved.

In the case of the water molecule, PES of the lowest states of the molecular anion were accurately mapped by Werner et al. [7] with the multireference CI method, mostly in the linear geometry of the molecule¹. They noted that the anion state becomes unstable at geometries close to the equilibrium of the water molecule, but they found a shallow minimum in the direction towards the $\text{O}^- + \text{H}_2$ asymptote. The minimum is separated from the autodetachment region by a saddle. This shape of the potential may be responsible for existence of quasibound anion states that were observed by Koning and Nibbering [26]. This is a similar situation like that known in some diatomic molecules [27], where the metastable states in the outer potential minimum are also closely related to oscillatory structures in the vibrational excitation cross sections [25,28].

Our goal is first to map the global structure of PES of both the lowest anion and neutral state of the water molecule and to localize the intersection of these two surfaces. We will also perform electron-molecule scattering calculations inside the autodetachment region, where the anion state disappears in the electronic continuum. Then we would like to construct the diabatic representation of the crossing between the anion and neutral state, i.e. we want to construct the nonlocal model for the reaction dy-

namics [23]. With the help of the nonlocal model, our final goal is to clarify the open questions mentioned above, namely:

1. We would like to search for the DA signal near the threshold in scattering of electrons from water molecules in ro-vibrational excited states.
2. We want to look at the exact shape of the threshold peaks or possible boomerang oscillations in the VE cross sections including the excited target states of H_2O .
3. We want to characterize the metastable states of H_2O^- , including their lifetime.
4. Finally we want to study the dynamics of $\text{O}^- + \text{H}_2$ and $\text{OH}^- + \text{H}$ collisions including the associative detachment channel.

To achieve these goals we start by looking at the global structure of the lowest PES of both H_2O and H_2O^- obtained from ab initio quantum chemistry calculations and we also discuss the results of electron-molecule scattering calculations in this paper. To obtain consistent data from both calculations is not an easy task, because the scattering calculations can usually be done only at a much lower level of electron correlation. Here we propose a method how to find a scattering model which can be used in the R -matrix calculations to get scattering data consistent with accurate quantum chemistry results for PES. The method is based on comparison of the PES in the region where electron submerges in the continuum. These steps are a preparation phase for construction of the full 3-dimensional nonlocal resonance model of the water molecular anion which we will attempt in a subsequent paper.

The paper is organized in the following way. After a short discussion of the previous calculations we describe the details of our multireference configuration interaction (MRCI) calculation of PES in Section 2. This section also contains the details of the R -matrix calculations. The actual results are discussed in Section 3 starting by an overview of the 3D PES data. Tuning of the R -matrix calculations is then demonstrated on two one-dimensional sections through PES in the region of the crossing between neutral and anion states. After the R -matrix model is carefully chosen, taking into account consistency with the PES calculations, we discuss the electron scattering eigenphase sums obtained along the same one-dimensional sections. The paper is concluded by Section 4 where we discuss the future steps needed to construct the nonlocal model from the present data.

2 Details of the calculation

There were several previous theoretical studies on low-energy electron scattering from the water molecule. These calculations are usually restricted to the static-exchange or static-exchange plus polarization approximations (see for example [29,30]) and most of the studies are done for molecular geometries near the equilibrium configuration of the neutral water molecule (see [31,32] and references therein). For accurate description of the $\text{O}^- + \text{H}_2$ and

¹ A very detailed study of Haxton et al. [2,5] was focussed on PES of the higher lying Feshbach resonances.

$\text{OH}^- + \text{H}$ channels, we need electron scattering calculations for a large range of highly distorted geometries of the H_2O molecule. Haxton and collaborators [2,5] performed such studies using complex-Kohn electron-molecule scattering calculations to obtain the decay widths of the Feshbach resonance states of H_2O^- for a large range of molecular geometries. They also constructed the global PES for these states using configuration interaction calculations on the restricted Hilbert space. However, their focus was on higher energies and they did not study the lowest anion state.

To our knowledge there was only one previous serious attempt to construct global PES for the ground state water molecular anion using ab initio quantum chemistry calculations with a high level of description of correlation energy. This was done by Werner et al. [7] who restricted their study mostly to the linear geometry, and a few one dimensional sections. In our previous paper [11] we extended their work to map globally the potential energy surface for the lowest electronic singlet state of the neutral H_2O molecule and for the lowest three electronic doublet states connected to the $\text{O}^-(^3\text{P}) + \text{H}_2(\text{X}^1\Sigma_g^+)$ asymptote in the region where these states are bound. The calculations have been done using the MRCI method starting from multi-configuration self-consistent field (MCSCF) method with 8 or 9 electrons in 10 active orbitals with the aug-cc-pVTZ basis. This method was sufficiently accurate to get the first insight to the dynamics of the $\text{O}^- + \text{H}_2$ reaction but we did not attempt to calculate fixed-nuclei scattering calculations consistent with these PES at that time. Our motivation in reference [11] was to explain the high cross section for the associative detachment process (1) and we did not present the calculated data in much detail. Here we discuss the potential energy surface of the ground anion state in more detail. Although in this paper we are interested especially in the ground state we have to calculate all three states because they are coupled through the Renner-Teller coupling and a conical intersection as explained in reference [11] and in Section 3. All quantum chemistry calculations have been done with MOLPRO package [33,34] using the internally contracted MRCI method [35] starting from MCSCF [36,37] with standard bases of Dunning [38].

The fixed-nuclei scattering calculations have been done using the R -matrix method [39] as implemented in the UK R -matrix suite of codes [40,41]. Unfortunately the active space used in our previous calculations turned out to be too large for practical fixed-nuclei scattering calculations. Therefore, one of goals of this paper is to find a smaller active space which would describe the shape of the target PES sufficiently accurately at least in the autodetachment region (and in its near neighborhood) and for which the scattering calculations would be feasible for many geometries. Within the UK R -matrix suite of codes the target molecule (H_2O) is usually described using the MCSCF method, particularly the complete active space self-consistent field (CASSCF) method. We used this method with the lowest $1a'$ molecular orbital closed and with 6–10 active molecular orbitals. We will denote such a method CAS(1c,na) for short. As a basis for the target calculations

we used the cc-pVTZ basis of Dunning [38] which is sufficient for the neutral water molecule in the autodetachment region. The aug-cc-pVTZ basis with diffuse functions cannot be used in the R -matrix electron scattering calculations due to problems with linear dependency with the continuum basis.

There are several possibilities how to construct models for fixed-nuclei electron scattering using the UK R -matrix suite. In this work we do not consider the static-exchange and static-exchange plus polarization methods because within these methods the target molecule is described by a single-determinant Hartree-Fock (HF) wave function which is not suited for calculations further from the equilibrium geometry (see Sect. 3 for an example). Therefore we compare only results obtained using the close-coupling models in which several target states can be included in the expansion of the scattering wave function (see [39] and references therein for details). In our scattering calculations the target wave functions were determined using CASSCF method with 1 closed and 6 active (valence) orbitals, CAS(1c,6a). A little bit larger active spaces can also be used in practical calculations but in this paper we want only to illustrate a method which enables us to find a scattering model consistent with PESs from large quantum chemistry calculations. Therefore only results obtained for this relatively small active space will be shown. The L^2 functions included in the close-coupling expansion of the scattering wave function in the inner region of the R -matrix method (again see [39] for details) were of the form

$$(1a')^2(\text{CAS})^9, \text{ and } (1a')^2(\text{CAS})^8(\text{virtual})^1 \quad (4)$$

where CAS symbolizes all $\{2a', 3a', 1a'', 4a', 5a', 6a'\}$ orbitals of the active space and *virtual* stand for chosen target virtual orbitals. Depending on the number of these virtual orbitals and the number of target states included in the scattering wave function expansion we can increase or decrease a level of electron correlation included in the scattering calculations relative to electron correlation included in the target description. This freedom allows us to tune the relative energy of neutral and ion PES. All scattering calculations were done with the continuum basis for the R -matrix sphere $r = 10$ a.u.

When comparing different methods and models it is not feasible to compute the whole three-dimensional PES globally within each approach. Therefore in this paper, we decided to look only at two one-dimensional sections. The first one which is important for assessment of the quality of the neutral H_2O PES is symmetric stretch near the experimental equilibrium geometry². For this section we fixed the angle $\theta_{\text{HOH}} = 104.4^\circ$ and varied the O-H distance r in the interval 1.0–4.0 a.u. The second section is the linear configuration of the $\text{H} + \text{OH}^-$ channel for which we fixed the OH^- distance to $r_{\text{OH}_1} = 1.829$ a.u. (the equilibrium distance of OH^- obtained with the MRCI method) and varied the second O-H distance r_{OH_2} in the interval 1.0–4.0 a.u. These ranges cover the region where the anion state dissolves in the continuum.

² The bond distances $r_{\text{OH}_1} = r_{\text{OH}_2} = 0.958 \text{ \AA}$ and angle $\theta_{\text{HOH}} = 104.4776$ [42]

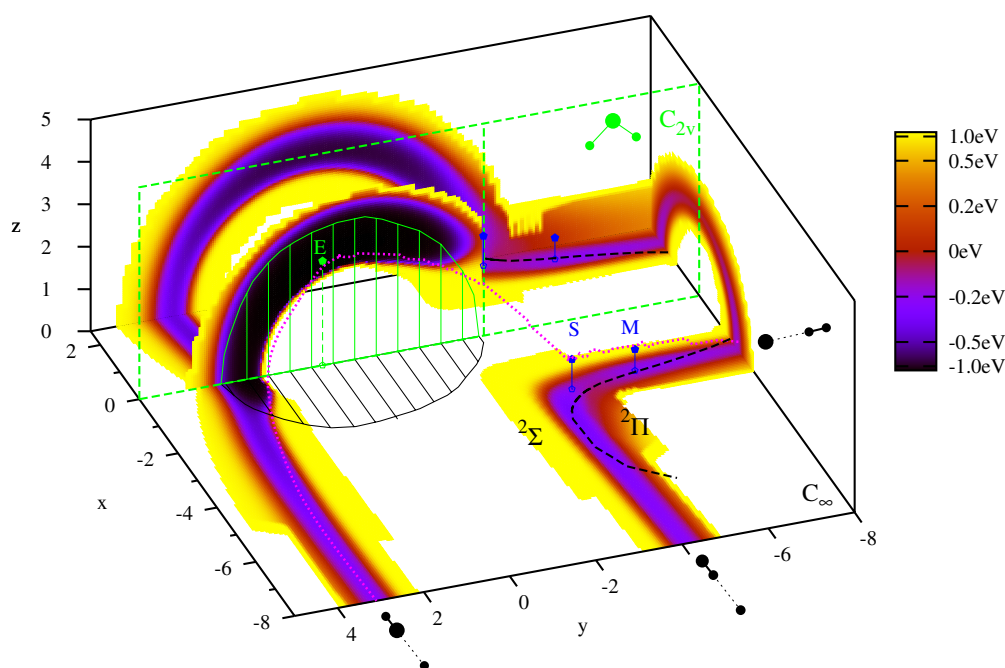


Fig. 1. The potential energy surface for the ground state of the water anion in the internal coordinates of Johnson [43]. The zero is shifted to the asymptotic energy in $\text{H}_2 + \text{O}^-$ channel (see the color code right of the figure). The plane $z = 0$ corresponds to the linear geometry (the $C_{\infty v}$ symmetry group). The directions to the $\text{O}^- + \text{HH}$, $\text{OH}^- + \text{H}$ and $\text{HO}^- + \text{H}$ asymptotes are indicated at the lower and right edges with black dots. The black dashed line marks the position of the conical intersection, where the symmetry of the ground state changes from ${}^2\Pi$ to ${}^2\Sigma^+$. The plane $x = 0$ (corresponding to the C_{2v} symmetry group) is shown with the green dashed rectangle. Special points E (the equilibrium geometry of the neutral H_2O), S (saddle point) and M (minimum) are connected with their projection to $z = 0$ plane. The dotted line shows the minimum energy reaction path from the $\text{O}^- + \text{HH}$ to $\text{HO}^- + \text{H}$ channels. It crosses the autodetachment area, which is filled with the net of solid lines.

3 Discussion of results

The overview of the results for the potential energy of the water anion ground state obtained with the above described MRCI calculations is shown in Figure 1 in the hyperspherical coordinates of Johnson [43] (see the appendix). All distances are given in units of the Bohr radius and energies in eV (see the color key in the inset). The potential energies are shifted so that the zero energy corresponds to the asymptotic energy of infinitely separated O^- and H_2 ($X^1\Sigma_g^+$). We show the section through PES in the direction towards this asymptote in the plane $y = -8$. It is dominated by interaction of the charged O^- anion with the quadrupole of the H_2 molecule. This interaction is strongest in the $z = 0$ plane. The $z = 0$ plane in the Johnson coordinates corresponds to linear geometries of the molecule. As we discussed already in reference [11] there are three states connected to the $\text{O}^-({}^3\text{P}) + \text{H}_2$ asymptote which are coupled through the Renner-Teller coupling and conical intersection. Two of the three states form a Renner-Teller pair that becomes a degenerate ${}^2\Pi$ -state in the linear geometry. The third state has ${}^2\Sigma^+$ symmetry in the linear geometry. The Renner-Teller pair crosses with the ${}^2\Sigma^+$ state. This crossing is marked in Figure 1 with the dashed line in the $z = 0$ plane. The ${}^2\Pi$ state has lower energy on the right side of this line, whereas the ${}^2\Sigma^+$ state is lower in the rest of the plane. For $z > 0$ the three states split and the lowest of them has A'

symmetry. This is the state which we follow in its crossing with the PES of the neutral molecule. The area where the anion state lies above the neutral PES is marked by a net of solid lines in Figure 1 (the autodetachment region). Three geometries of special interest are also marked by letters in the figure. These are the outer minimum (M) and the saddle point (S) discovered by Werner et al. [7] and the equilibrium (E) geometry of the neutral molecule. We found that the minimum and the saddle point lie a little bit off the linear geometry at $z > 0$. Also shown is the minimum energy path – the dotted line that passes through all of the special points. We used this reaction path in reference [11] to plot the PES for interpretation of the associative detachment measurement in $\text{O}^- + \text{H}_2$ collisions. The reaction path comes close to the equilibrium geometry (E) located in the plane $x = 0$. This plane corresponds to geometries with C_{2v} symmetry. All three states that are degenerate in the $\text{O}^- + \text{H}_2$ asymptote split in this plane and only the lowest A' state falls down into the autodetachment region from all directions.

In the next paragraph we study PES for both the ground neutral and anion states along two one dimensional sections mentioned above. The symmetric stretch section points radially from center $(x, y, z) = (0, 0, 0)$ through the point (E) in Figure 1. The second section along $\text{H} + \text{OH}^-$ asymptote is located in the $z = 0$ plane close to the dotted reaction path in the bottom left corner of the figure.

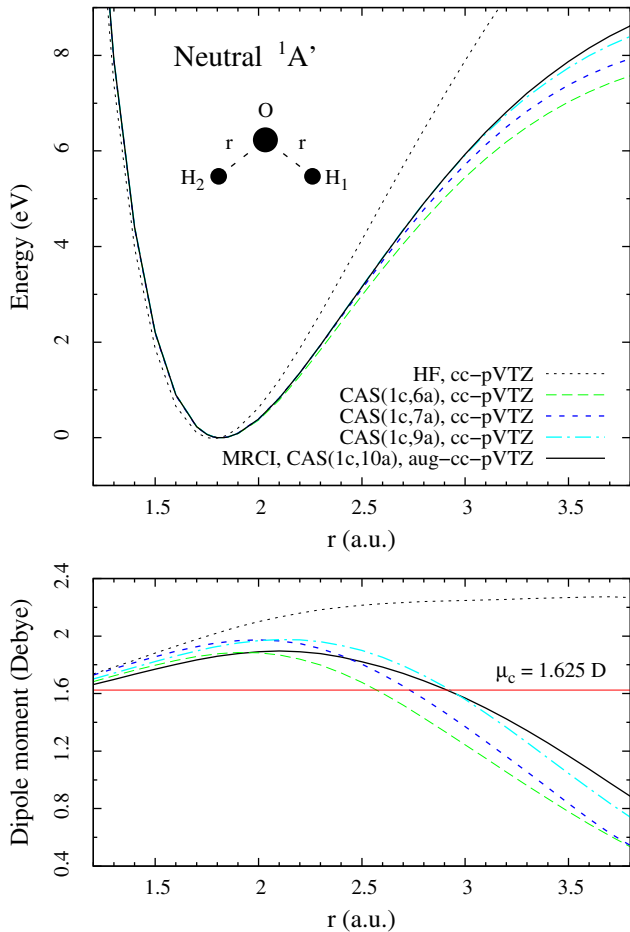


Fig. 2. Comparison of the potential energy (upper panel) and dipole moment functions (lower panel) of the neutral molecule calculated using the HF, CASSCF and MRCI methods for the symmetric stretch through the equilibrium geometry, the angle HOH is 104.4° . The results for several CASSCF active spaces are shown which can be used to describe the target molecule in the R -matrix scattering calculations.

The PES described above and shown in Figure 1 is used as the reference for tuning of the scattering R -matrix calculations.

3.1 Potential energy surfaces

We start by looking at the performance of different methods for the ground state of the neutral H_2O . In Figure 2, the potential energy (upper panel) and dipole moment functions (lower panel) for the symmetric stretch around the equilibrium geometry are shown for several different CASSCF active spaces in the cc-pVTZ basis and compared with the HF method and the results from MRCI calculations with the aug-cc-pVTZ basis. For better comparison, all potential energy surfaces in this and the following figures were shifted to be zero at geometry $r_{\text{OH}_1} = r_{\text{OH}_2} = 1.81$ a.u., $\theta_{\text{HOH}} = 104.4^\circ$ which is near the experimental equilibrium. Values of energies at this point for all used methods can be found in Table 1.

Table 1. Energies of the neutral H_2O molecule calculated by various quantum chemical methods at the geometry $r_{\text{OH}_1} = r_{\text{OH}_2} = 1.81$ a.u., $\theta_{\text{HOH}} = 104.4^\circ$ which is near the experimental equilibrium. These values are used to shift the potential energy surfaces to compare their shape near the equilibrium. We should note that actual minima for various methods lie at slightly different geometries.

Method	Basis	Energy/a.u.
HF	cc-pVTZ	-76.057121
CAS(1c,6a)	cc-pVTZ	-76.110443
CAS(1c,7a)	cc-pVTZ	-76.135976
CAS(1c,9a)	cc-pVTZ	-76.203656
MRCI, CAS(1c,10a)	aug-cc-pVTZ	-76.337586

Figure 2 clearly demonstrates the insufficiency of the Hartree-Fock model to describe the target H_2O molecule for electron-molecule scattering calculations. First, as compared to the MRCI result (solid lines) the Hartree-Fock (dotted curves) potential energy well is too narrow, which would lead to wrong positions of vibrational states. Second, the dependence of the dipole moment on the symmetric stretch coordinate is qualitatively wrong. While the Hartree-Fock dipole moment stays overcritical, the correct value of the dipole decreases for the large symmetric stretch. The value of the dipole moment is very important for the correct description of the onset of the autodetachment in the scattering calculations [44]. The dashed curves show the results of calculations on the level of correlation that is affordable in the R -matrix codes. These curves are sufficiently close to the results of the MRCI calculations.

3.2 Fixed-nuclei electron scattering

In order to find a suitable model for the fixed-nuclei electron scattering consistent with PES obtained from the large quantum chemistry calculations, at least in the vicinity of the onset of the autodetachment region, we propose to use the following approach. Within the UK R -matrix suite of codes it is possible not only to run scattering calculations but also to compute ion bound states using the same close-coupling model as in scattering runs. We can therefore perform calculations of ion bound states at several geometries for close-coupling models with a different number of target states and/or virtual orbitals included in the model and compare them with large MRCI calculations. Because for electron scattering only a relative position of the neutral and ion PES is crucial, not absolute energies, the best scattering models are those which reproduce the boundary of the autodetachment region reasonably well. Such models can then be used for scattering calculations inside the autodetachment region.

Here we demonstrate this approach by calculations performed along two sections described in Section 2. Results for the symmetric stretch are shown in Figure 3 and these for the HO-H stretch are in Figure 4. For both sections we plotted the lowest $^1A'$ state of H_2O (black solid curve) and the lowest $^2A'$ state of H_2O^- (red solid curve with diamonds) up to the boundary of the

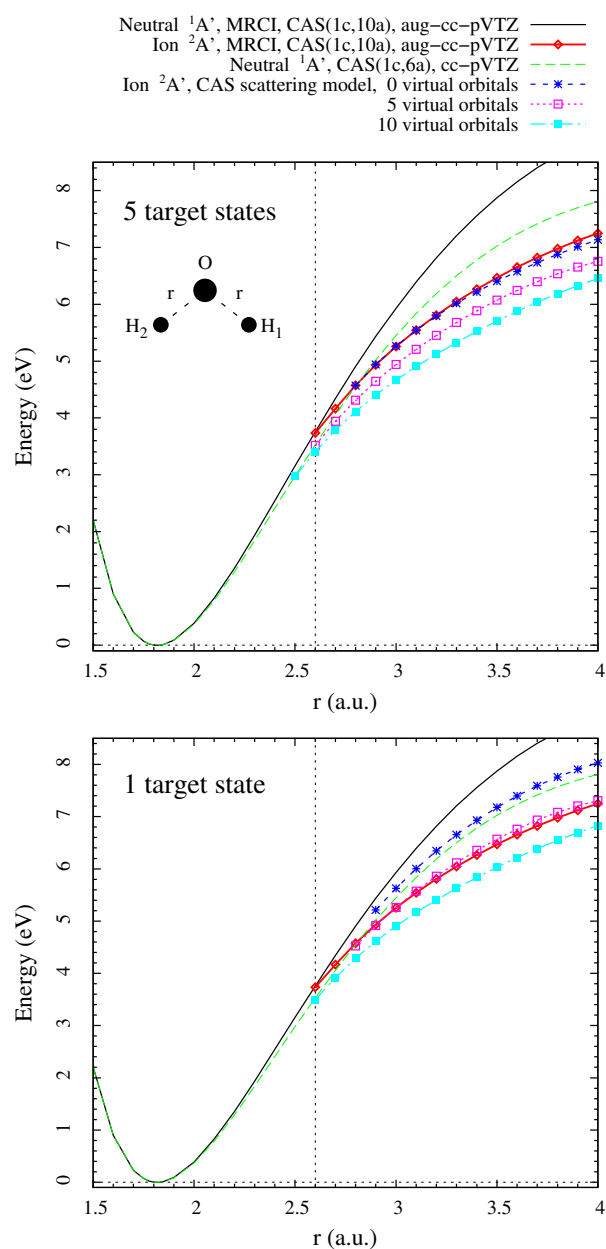


Fig. 3. Comparison of various R -matrix scattering CAS models with PESs obtained by MRCI method for the symmetric stretch through the equilibrium geometry, the angle HOH is 104.4° . The close-coupling model included 5 target states (upper panel) or 1 target state (lower panel) and a different number of virtual orbitals.

autodetachment region marked by a vertical dashed line, as determined from the large MRCI calculations with the aug-cc-pVTZ basis. In the upper panels of the figures we compare the MRCI results with the target (green dashed curve) and ion bound states obtained using the close-coupling CAS(1c,6a) models with 5 target states and 0, 5, and 10 virtual states. In the lower panels we show results for the same models but only with 1 target state included. We should note that the model with 1 target state and 0 virtual orbitals does not give an ion bound state with

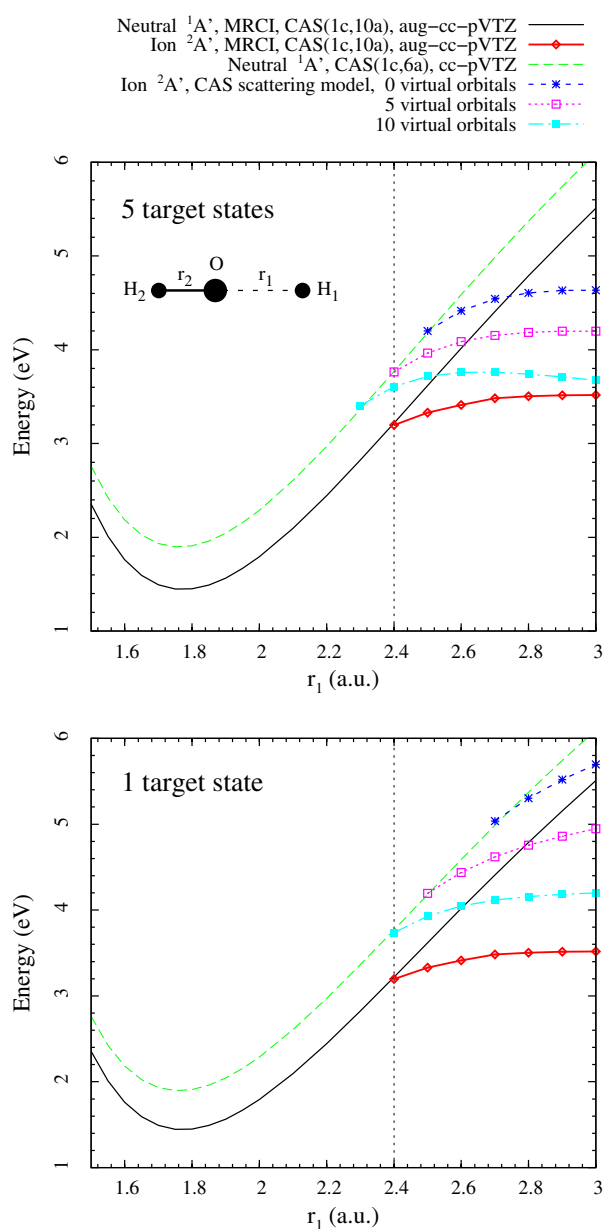


Fig. 4. The same as in Figure 3 but for the linear HO-H stretch where the HO bond is $r_2 = 1.829$ a.u.

energy below the target ground state for the symmetric stretch at studied geometries and the data shown in Figure 3, lower panel, represent actually discretization of the electron continuum. In both cases and for both sections we can find a scattering model which gives the crossing of the target and ion potential curves at almost the same geometry as for the MRCI potential curves, namely for 5 target states the best choice is 5 virtual orbitals and for 1 target state 10 virtual orbitals.

Eigenphase sums for $2A'$ symmetry for these two *optimal* scattering models for several geometries are shown in Figure 5 for the symmetric stretch and in Figure 6 for the HO-H stretch. Behavior of eigenphase sums close to zero energy is strongly influenced by the presence or absence of

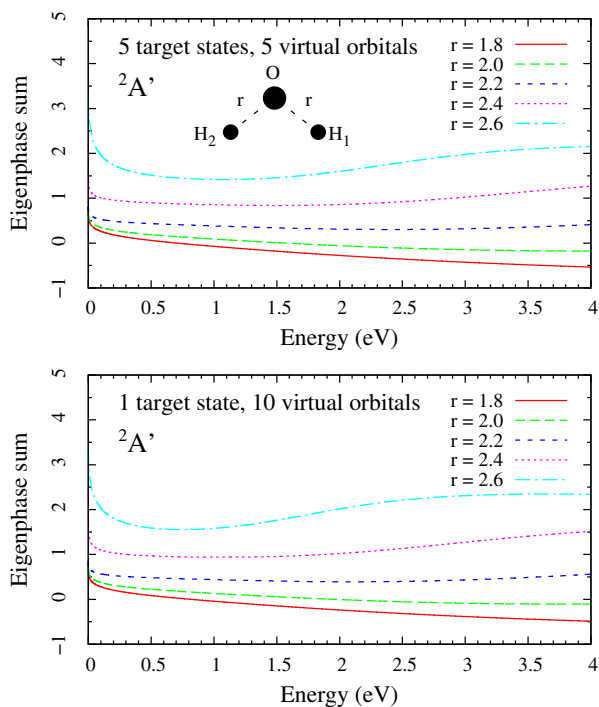


Fig. 5. Fixed-nuclei eigenphase sums for ${}^2A'$ symmetry calculated at several OH distances for the symmetric stretch geometry for two scattering CAS models which are in a good agreement with MRCI PES.

the ion bound state together with the permanent dipole moment which is supercritical around the equilibrium geometry. The eigenphase sums therefore diverge logarithmically at threshold³ in Figure 5 while they converge to finite value in Figure 6 where the size of the dipole is subcritical. The threshold value in Figure 6 increases by π when the bound state is formed around $r_1 = 2.4$ (see [45] for detailed discussion of phaseshifts for dipole potential with additional electron-binding potential). Note that there is no sharp resonance in the eigenphase sums corresponding to the lowest ${}^2A'$ state (2A_1 in C_{2v} symmetry) of H_2O^- after this state disappears as a bound state. This is no obstacle to construct a nonlocal model (see [23,46] and references therein). The broad resonance appearing for the symmetric stretch at $r > 2.2$ is related to another higher ${}^2A'$ state which is the 2B_1 state in C_{2v} symmetry. Eigenphase sums for two chosen models differ only slightly and both models could be used for the construction of the nonlocal model for nuclear dynamics. The difference between results for two (or more) such models could be used to estimate uncertainty in the final cross sections.

4 Conclusions and future prospects

We have studied the global structure of the ground state of the water anion. Using the MRCI method we have cal-

³ The logarithmic divergence is difficult to distinguish from $C - x^\alpha$ behavior for $\alpha \ll 1$ in the scale used in the figures.

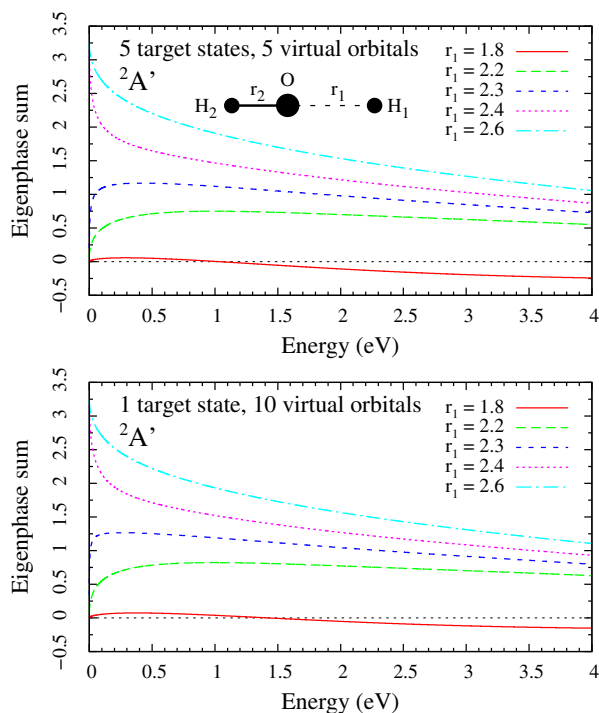


Fig. 6. The same as in Figure 5 but for the linear HO-H stretch where the length of the other HO bond is $r_2 = 1.829$ a.u.

culated the potential energy of this anion state for many molecular geometries covering the range from the equilibrium geometry of the neutral to the asymptotic region of both the $OH^- + H$ and $O^- + H_2$ channels.

For two one dimensional sections in the full 3D configuration space of molecular geometries we have shown that it is possible to find a close-coupling model for fixed-nuclei scattering calculations consistent with the potential energy surfaces from large quantum chemistry calculations. This consistency is usually achieved by tuning of the positions of the narrow resonance states. Here we have demonstrated that it is possible even when there is no such resonance state by looking in the crossing region of PES of anion and neutral states. Since the position can be tuned by two parameters (number of target states and number of virtual states used in the expansion of the scattering state) we were able to find two models consistent with higher level quantum chemistry calculations. The scattering eigenphase sums in both models agree rather well. Remaining difference can still be used in future estimates of the error of the calculation.

In future we will check the consistency of the data also for other geometries near the boundary of the autodetachment region and we will use the scattering data for construction of the global nonlocal model of the nuclear dynamics of the H_2O^- system. To define the nonlocal resonance model we need the potential $V_0(\mathbf{X})$ of the neutral molecule, the potential $V_d(\mathbf{X})$ of the discrete state (anion) and the coupling matrix element $V_{d\epsilon}(\mathbf{X})$ between the discrete state and the electron continuum (ϵ is the electron energy). Both V_0 and V_d far from autodetachment

region are calculated directly as described above. The coupling matrix element V_{de} and the potential V_d inside autodetachment region are fitted to reproduce the electron scattering data with fixed \mathbf{X} in similar way as described for example in references [23,24]. The only difference between the polyatomic and the diatomic case is that the parameter X for diatomic molecule is real number (distance of the nuclei) while we need the three component vector \mathbf{X} for the case of triatomic molecule. This difference poses no principal difficulty in constructing the model (see [47,48] where a generalization of the method diatomics-in-molecules was used to construct a nonlocal model for H_3^-), although the treatment of the nuclear dynamics will be much more complicated and time consuming.

Once the model is constructed it can directly be used for the description of the vibrational excitation of the water molecules by low-energy electrons and for calculation of the dissociative attachment into the $\text{OH}^- + \text{H}$ channel near the threshold. For description of the dissociation to the $\text{O}^- + \text{H}_2$ channel and for calculation of properties of the long-lived H_2O^- states we also have to construct a model of nonadiabatic dynamics of the Renner-Teller doublet coupled through the conical intersection with the ground anion state.

Appendix: Hyperspherical coordinates of Johnson

The results for the ground state potential energy surface and the autodetachment region are presented in Figure 1 in the hyperspherical coordinates of Johnson [43]. These coordinates are based on the mass scaled Jacobi coordinates

$$\mathbf{r} = (\mathbf{x}_1 - \mathbf{x}_2)/d_0, \quad (\text{A.1})$$

$$\mathbf{R} = d_0[\mathbf{x}_0 - \frac{1}{2}(\mathbf{x}_1 + \mathbf{x}_2)], \quad (\text{A.2})$$

where \mathbf{x}_1 , \mathbf{x}_2 and \mathbf{x}_0 are the position vectors of two hydrogen atoms and the oxygen atom respectively and the mass scaling factor d_0 is defined in terms of masses of hydrogen and oxygen as follows

$$M = m_{\text{H}} + m_{\text{H}} + m_{\text{O}}, \quad (\text{A.3})$$

$$\mu^2 = m_{\text{H}}m_{\text{H}}m_{\text{O}}/M, \quad (\text{A.4})$$

$$d_0^2 = \frac{m_{\text{O}}}{\mu} \left(1 - \frac{m_{\text{O}}}{M}\right). \quad (\text{A.5})$$

The Johnson coordinates then read

$$x = 2\mathbf{r} \cdot \mathbf{R}/\rho, \quad (\text{A.6})$$

$$y = (\mathbf{r}^2 - \mathbf{R}^2)/\rho, \quad (\text{A.7})$$

$$z = 2|\mathbf{r} \times \mathbf{R}|/\rho, \quad (\text{A.8})$$

with the hyperradius

$$\rho^2 \equiv \mathbf{r}^2 + \mathbf{R}^2 = x^2 + y^2 + z^2. \quad (\text{A.9})$$

Following facts are important for the understanding of the plots in these coordinates:

- The plane $x = 0$ contains configurations with the vector \mathbf{r} perpendicular to \mathbf{R} , i.e. distance of both hydrogen atoms from the oxygen is the same. This is characteristic for the C_{2v} symmetry (the same as the ground state configuration of the neutral H_2O molecule).
- The plane $z = 0$ contains configurations with the linear ($C_{\infty v}$) geometry since $\rho z/4$ is the area of the triangle defined by the three (H, H, O) atoms.
- Scaling of all distances in the H_2O molecule by the same factor scales also all x , y , z coordinates by the same factor, i.e. the symmetric stretch vibrations happen along the line pointing radially from the center of the x , y , z coordinate system.
- All two body asymptotes (configurations with two atoms staying close to each other and one atom escaping to the infinity) stay near to the $z = 0$ plane, but far from the origin.

This paper is dedicated to Michael Allan, our dear friend and collaborator, on the occasion of his retirement after many years of outstanding research in atomic and molecular physics. The work is supported by grant agency of Czech Republic under contract number GACR 16-17230S.

References

1. Y. Itikawa, N. Mason, J. Phys. Chem. Ref. Data **34**, 1 (2005)
2. D.J. Haxton, Ph.D. thesis, University of California, Berkeley, 2006
3. R.N. Compton, L.G. Christophorou, Phys. Rev. **154**, 110 (1967)
4. C.E. Melton, J. Chem. Phys. **57**, 4218 (1972)
5. D.J. Haxton, C.W. McCurdy, T.N. Rescigno, Phys. Rev. A **75**, 012710 (2007)
6. D.J. Haxton, T.N. Rescigno, C.W. McCurdy, Phys. Rev. A **75**, 012711 (2007)
7. H.-J. Werner, U. Manz, P. Rosmus, J. Chem. Phys. **87**, 2913 (1987)
8. J. Fedor, P. Cicman, B. Coupier, S. Feil, M. Winkler, K. Gluch, J. Husarik, D. Jaksch, B. Farizon, N.J. Mason, P. Scheier, T.D. Märk, J. Phys. B **39**, 3935 (2006)
9. J.L. Mauer, G.J. Schultz, Phys. Rev. A **7**, 593 (1972)
10. P. Jusko, Š. Roučka, R. Plašil, J. Glosik, Int. J. Mass Spectrom. **352**, 19 (2013)
11. P. Jusko, Š. Roučka, D. Mulin, I. Zymak, R. Plašil, D. Gerlich, M. Čížek, K. Houfek, J. Glosik, J. Chem. Phys. **142**, 014304 (2015)
12. J.C. Howard, F.C. Fehsenfeld, M. McFarland, J. Chem. Phys. **60**, 5086 (1974)
13. M. Čížek, J. Horáček, W. Domcke, J. Phys. B **31**, 2571 (1998)
14. M. Allan, S.F. Wong, Phys. Rev. Lett. **41**, 1791 (1978)
15. J. Horáček, M. Čížek, K. Houfek, P. Kolorenč, W. Domcke, Phys. Rev. A **70**, 052712 (2004)
16. R. Čurík, J.P. Ziesel, N.C. Jones, T.A. Field, D. Field, Phys. Rev. Lett. **97**, 123202 (2006)
17. M. Allan, O. Moreira, J. Phys. B **35**, L37 (2002)
18. G. Seng, F. Linder, J. Phys. B **9**, 2539 (1976)

19. K. Rohr, J. Phys. B **10**, L735 (1977)
20. H. Hotop, M.-W. Ruf, M. Allan, I.I. Fabrikant, Adv. At. Mol. Opt. Phys. **49**, 85 (2003)
21. K. Rohr, F. Linder, J. Phys. B **8**, L200 (1975)
22. O. Schafer, M. Allan, J. Phys. B **24**, 3069 (1991)
23. W. Domcke, Phys. Rep. **208**, 97 (1991)
24. W. Domcke, C. Mündel, J. Phys. B **18**, 4491 (1985)
25. M. Čížek, J. Horáček, M. Allan, W. Domcke, Czech. J. Phys. **52**, 1057 (2002)
26. L.J. de Koning, N.M.M. Nibbering, J. Am. Chem. Soc. **106**, 7971 (1984)
27. M. Čížek, J. Horáček, W. Domcke, Phys. Rev. A **75**, 012507 (2007)
28. M. Čížek, J. Horáček, Int. J. Mass Spectrom. **280**, 149 (2009)
29. O. Moreira, D.G. Thompson, B.M. McLaughlin, J. Phys. B **34**, 3737 (2001)
30. M.A. Khakoo, C. Winstead, V. McKoy, Phys. Rev. A **79**, 052711 (2009)
31. A. Faure, J.D. Gorfinkiel, J. Tennyson, J. Phys. B **37**, 801 (2004)
32. R. Zhang, A. Faure, J. Tennyson, Phys. Scr. **80**, 015301 (2009)
33. H.-J. Werner, P.J. Knowles, G. Knizia, F.R. Manby, M. Schütz, WIREs Comput. Mol. Sci. **2**, 242 (2012)
34. H.-J. Werner, P.J. Knowles, G. Knizia, F.R. Manby, M. Schütz and others, MOLPRO, version 2012.1, a package of ab initio programs, see <http://www.molpro.net>
35. P.J. Knowles, H.-J. Werner, Theor. Chim. Acta **84**, 95 (1992)
36. H.-J. Werner, P.J. Knowles, J. Chem. Phys. **82**, 5053 (1985)
37. P.J. Knowles, H.-J. Werner, Chem. Phys. Lett. **115**, 259 (1985)
38. T.H. Dunning, Jr., J. Chem. Phys. **90**, 1007 (1989)
39. J. Tennyson, Phys. Rep. **491**, 29 (2010)
40. L.A. Morgan, J. Tennyson, C.J. Gillan, Comput. Phys. Commun. **114**, 120 (1998)
41. J.M. Carr, P.G. Galiatsatos, J.D. Gorfinkiel, A.G. Harvey, M.A. Lysaght, D. Madden, Z. Mašín, M. Plummer, J. Tennyson, H.N. Varambhia, Eur. Phys. J. D **66**, 58 (2012)
42. NIST Computational Chemistry Comparison and Benchmark Database, NIST Standard Reference Database Number 101, Release 17b, September 2015, edited by Russell D. Johnson III, <http://cccbdb.nist.gov>
43. B.R. Johnson, J. Chem. Phys. **73**, 5051 (1980)
44. J. Horáček, M. Čížek, W. Domcke, Theor. Chem. Acc. **100**, 31 (1998)
45. H. Estrada, W. Domcke, J. Phys. B **17**, 279 (1984)
46. M. Čížek, J. Horáček, M. Allan, I.I. Fabrikant, W. Domcke, J. Phys. B **36**, 2837 (2003)
47. A.K. Belyaev, A.S. Tiukanov, W. Domcke, Phys. Rev. A **65**, 012508 (2001)
48. A.K. Belyaev, A.S. Tiukanov, W. Domcke, Chem. Phys. **325**, 378 (2006)